Screening for New Interaction Partners for a Group IIB Intron Ribozyme with Surface Plasmon Resonance Imaging Coupled to MALDI Mass Spectrometry

Ulrike Anders[†,‡], Maya Gulotti-Georgieva[§,‡], Susann Zelger-Paulus[§], Fatima-Ezzahra Hibti[Ω], Chiraz Frydman[Ω], Detlev Suckau[Δ], Roland K.O. Sigel[§] and Renato Zenobi[,†]*

[†]Department of Chemistry and Applied Biosciences, ETH Zurich, Vladimir-Prelog-Weg 3, CH-8093 Zurich, Switzerland
[§]Department of Chemistry, University of Zurich, Winterthurerstr. 190, CH-8057 Zurich, Switzerland
[Ω]Horiba France S.A.S., Avenue de la Vauve – Passage Jobin Yvon, CS 45002 – F-91120 Palaiseau, France
[Δ]Bruker Daltonics, Fahrenheitstr. 4, D-28359 Bremen, Germany
[‡]These authors contributed equally to this work.

**Corresponding author: Renato Zenobi, e-mail: zenobi@org.chem.ethz.ch*

Running title: *Screening for New Interaction Partners*

Keywords: *group IIB intron, RNA, Mss116, SPRi, MALDI MS, screening, non-targeted*

ABSTRACT

RNA maturation is a highly regulated process whose precision is indispensable for the correct transfer of genetic information and, thus, the survival of any living organism. While in higher eukaryotes, this process is known to be assisted by the spliceosome, a very complex system assembled from numerous proteins, in bacteria splicing is catalyzed by ribozymes only. In lower eukaryotes however, e.g., yeast, RNA maturation is also expected to be less complex or simplified. Here, we focus on the mitochondrial group IIB intron RNA *Sc*.ai5γ from *Saccharomyces cerevisiae* (*Sc.*) and Mss116, a protein of the DEAD-box helicase family, known to play a crucial role in the *Sc*.ai5γ maturation pathway, acting as a co-factor *in vivo.* Although to date, only Mss116 has been described to be involved in the maturation of *Sc*.ai5γ, we hypothesize that the folding and splicing of *Sc*.ai5γ is regulated by more than one protein co-factor, i.e., that a complex or series of several proteins participate in folding and splicing the immature RNA correctly. For the identification of new potential *Sc*.ai5γ binders we coupled SPR imaging with matrix-assisted laser desorption/ionization mass spectrometry. This combination results in a powerful method to screen for specific RNA-binding proteins from complex mixtures, specifically lysate of the coarse mitochondrial fraction from yeast. Our results indicate that several proteins other than the well-known co-factor Mss116 interact with *Sc*.ai5γ, namely Dbp8, Prp8, Mrp13, and Cullin-3. With this novel approach, we report the identification of RNA-binding proteins from a crude yeast mitochondrial lysate in a non-targeted approach.

During protein biosynthesis, double-stranded deoxyribonucleic acid (DNA) consisting of coding regions (exons) and non-coding regions (introns) is transcribed into single-stranded pre-messenger ribonucleic acid (pre-mRNA). Subsequent RNA maturation includes splicing in which intronic RNA is excised while the exonic regions are joint together to form the mature RNA sequence. In the eukaryotic nuclear genome, this process is usually accomplished in a series of reactions catalyzed by the spliceosome - a complex of five snRNAs (small nuclear RNAs) and about 80 proteins (1,2). In lower eukaryotes, bacteria, and eukaryotic organelles, introns self-splice without the aid of this large RNA-protein complex. These catalytic RNAs, i.e., ribozymes, fold into a specific three-dimensional architecture capable of efficient self-splicing in two main steps.

The mitochondrial intron *Sc*.ai5γ from *Saccharomyces cerevisiae* (*Sc.*) belongs to the class of group IIB introns, natural catalytic RNAs or ribozymes, which share mechanistic and structural similarities with the spliceosome (1,3,4). Thus, it is believed that both mechanisms are evolutionary related and that group II introns are the phylogenetic ancestors of the spliceosomal machinery. While *in vitro* self-splicing of group II introns can be initiated by high concentrations of divalent metal ions (5,6), *in vivo* the ribozyme functions presumably as a stable ribonucleoprotein (RNP). The assisting protein is either encoded on the host intron (IEP), or as in the case of *Sc*.ai5γ, as part of the nuclear genome (7,8). Structurally, group II introns are highly conserved and display six domains (DI – DVI) radiating from a central wheel (9). Domain I (DI) is known to be the largest domain, which contains essential binding sites for the recognition of the exons as well as for its natural protein co-factor Mss116.

Mss116 is a DEAD-box helicase, and as such, a member of a large ATP-dependent enzyme family that is involved in various RNA metabolism (10,11). DEADbox proteins share a highly conserved core, consisting of nine preserved consensus motifs. However, the functional diversity among the family members arises from their remaining structural divergence. Functionally, Mss116 acts not only as an on-pathway intermediate chaperon, preventing kinetic traps during the RNA folding process, but it is also involved in a number of other activities such as strand annealing, conformational switching and charge neutralization (12-18). Mss116, as the only natural identified co-factor for *Sc*.ai5γ, is encoded in the nucleus. It is transported to the mitochondrial matrix via a signal-peptide, where it can bind to group I and II introns (13) and trigger their folding and subsequent splicing. The mechanism of Mss116-mediated splicing includes the resolution of misfolded structures by RNA unwinding and stabilization of correctly folded on-pathway intermediates. Fedorova *et al.* showed that the protein directly stimulates the RNA folding in an ATP-independent manner. Still, ATP is required for the protein turnover - the dissociation from incorrectly formed complexes and rebinding unfolded RNA (16). However, *in vitro* studies indicate

a low splicing efficiency (19), which is in line with our hypothesis that possibly other protein co-factors play a key role in the complete *Sc*.ai5γ maturation (14,20).

Although the interaction between *Sc*.ai5γ and Mss116 appears to be non-specific, a specific function of the protein, namely to act as an RNA co-factor, has been shown in the past by northern blotting (13). Equilibrium binding assays by Halls *et al.* (21) demonstrated that Mss116 is able to interact with other classes of introns as well, namely group I and group II introns, with dissociation constants (K_D) in the low nanomolar range, but the association and dissociation kinetic constants (k_{on} and k_{off}) were not determined. Mss116 is the only reported protein co-factor involved in *Sc*.ai5γ maturation, pre-mRNA splicing and ribosome assembly. However, the role of other mitochondrial proteins in *Sc*.ai5γ maturation remains unclear. While Mss116 was identified in a screen for nuclear mutants and their ability to grow in the presence or absence of introns (12), we demonstrate the ability of a hyphenated analytical method to discover further proteins that are involved in the RNA binding process.

A combination of several analytical methods would usually be required to identify binders and simultaneously determine the binding affinity, rendering work laborious, and time-consuming. The coupling of surface plasmon resonance imaging (SPRi) with mass spectrometry (MS) that was employed here combines quantitative analysis with unambiguous identification of captured target molecules in a single workflow (22-24). SPRi allows monitoring binding affinities and kinetics in real-time and at very low concentrations. SPR surfaces are reusable due to regeneration steps between different injections, which allow multiple measurements at different concentrations and, if necessary, various conditions. To identify the molecules captured on an SPR surface, matrix-assisted laser desorption/ionization mass spectrometry (MALDI MS) and peptide mass fingerprinting were implemented. By performing SPR and MALDI MS separately, as usually done (25-27), the throughput and sensitivity would be seriously limited due to the need for target elution, which often leads to sample loss and contaminations. Therefore, performing MALDI MS measurements directly on the SPR chip is beneficial (28,29). We have previously shown that the identity of interacting proteins not only from pure target solutions but also from cellular lysates could be established (30). The only other example reported is the study by Musso *et al*., who demonstrated the detection of α-amylase from human saliva by antibody-arrayed SPRi surfaces (31). To the best of our knowledge, screening for RNA binding proteins from cell lysates or specific compartments in, e.g., the mitochondria, with SPRi-MALDI MS, has never been performed before.

For unambiguous characterization of captured proteins, mass spectra of high quality are required. In the past, either self-digested peptides of trypsin dominated mass spectra and/or a small number of peptides were obtained from a single, purified injected protein (31-33). Increasing the efficiency of on-chip

proteolysis is therefore essential. Moreover, in order to avoid sample loss, both the MALDI and SPR analyses should be done on the same surface, which can be achieved by working with a MALDI MS compatible SPR chip. Thus, our study also includes improved on-chip digestion, yielding a sufficient number of peptide peaks for confident classification. High-quality MS and MS/MS of low protein concentrations in the fmol range from arrayed spots were obtained, resulting in increased protein identification reliability. We successfully analyzed the lysate of a coarse mitochondrial fraction from yeast and discovered four previously unknown *Sc*.ai5γ-interacting specific binders.

Results

Binding of Mss116 to ex^{41}-Sc.ai5γ-ex^{14}. To date, only the affinity of Mss116 to *Sc*.ai5γ has been determined (21), but the binding and unbinding kinetics remain unknown. Initially, SPRi measurements were performed to characterize the association and dissociation rate constants (k_{on} and k_{off}) of Mss116 to the intact ex^{41}-*Sc*.ai5γ-ex^{14}. These constants give an insight into the fast and specific interaction between both molecules and thus provide a better understanding of the biological system and exact mode of action. In a second step, we used SPRi-MALDI MS to identify additional RNA-binding proteins from a lysate of a coarse mitochondrial fraction, which required improved on-chip proteolysis.

To attach the RNA onto a surface, two different immobilization strategies were applied: a biotinylated DNA oligonucleotide was hybridized either to domain IV or the 5'exon of ex^{41}-*Sc*.ai5γ-ex^{14} (Figure 1 A). Hence, we examined whether the binding properties of Mss116 to the RNA are influenced due to a structurally different conformation or not and accordingly identify the better preferable immobilization position for optimal interaction. Injections of Mss116 at various concentrations (5-135 nM) showed a slow dissociation, which is not reaching the baseline level during the measuring time of 650 sec (Figure 1 B and Table 1). In agreement with previous investigations (34,35), the measured binding rates indicate a rapid binding of Mss116 (with a fast association rate constant) and a prolonged release (Figure 1 B and Table 1).

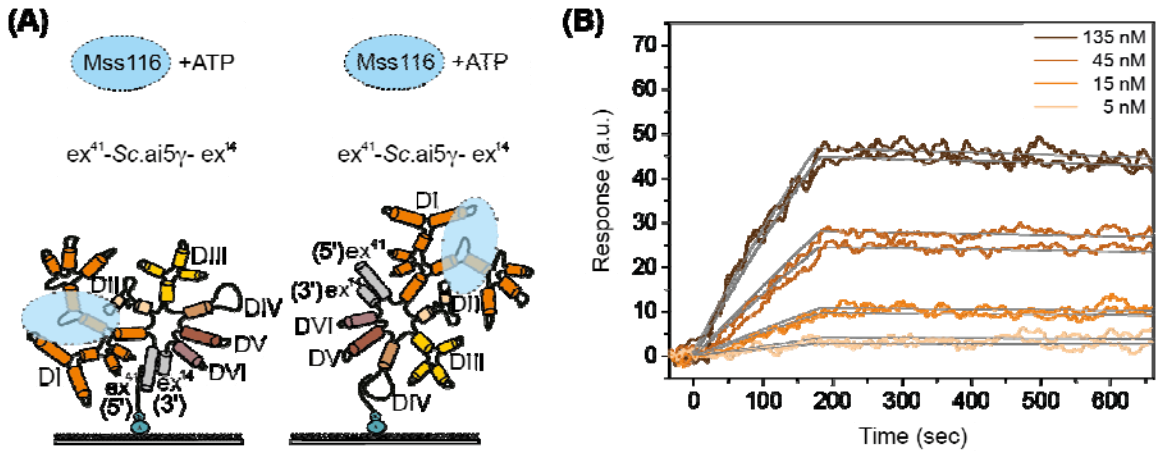

Figure 1. (A) Scheme of the secondary structure of ex^{41}-*Sc*.ai5γ-ex^{14} indicating the proposed binding site for Mss116 (blue) at a central three-way junction (κ-ζ) within DI (orange). Immobilization approaches via 5'exon (left) and DIV (right) are shown. **(B)** SPRi measurement of the group IIB intron ex^{41}-*Sc*.ai5γ-ex^{14} in the presence of ATP (10 µM) in running buffer and a concentration series of Mss116 (5-135 nM). Calculated K_D: 8.4 ± 0.7 nM (fits in grey).

Omitting ATP (10 µM) from the running buffer was found to have only little effects on the binding strength, with a K_D value in the low nanomolar range (Table 1 and Figure S3) as well as unaffected on- and off-rates. Variations in K_D by a factor of 3 to 4 obtained from biophysical experiments are within the tolerance range. Our findings on the low impact of ATP are in good agreement with previous results, where it was shown that the presence of ATP does not influence the protein-RNA binding strength (14). In contrast, it was reported that the release of Mss116 from the RNA is ATP-dependent (16,36). Therefore, all the following experiments were performed in the presence of ATP.

Table 1 Association (k_{on}) and dissociation (k_{off}) rate constants and K_D of the interaction between ex^{41}-*Sc*.ai5γ-ex^{14} and its co-factor Mss116 in the presence or the absence of ATP for both immobilization schemes (DIV and 5'exon). Standard deviations derive from two to four independent technical replicates.

Immobilization tag and position	ATP	k_{on} ($M^{-1}s^{-1}$)	k_{off} (s^{-1})	K_D (nM)
biotin – DIV	No	$5.76 \pm 0.07 \times 10^4$	$3.11 \pm 0.04 \times 10^{-4}$	5.40 ± 0.06
biotin – DIV	Yes	$1.20 \pm 0.10 \times 10^4$	$9.90 \pm 0.50 \times 10^{-5}$	8.40 ± 0.70
biotin – 5'exon	Yes	$3.00 \pm 0.10 \times 10^4$	$2.70 \pm 0.10 \times 10^{-4}$	9.10 ± 0.30
amine – DIV	Yes	$6.51 \pm 0.05 \times 10^4$	$1.35 \pm 0.01 \times 10^{-4}$	2.07 ± 0.02

We tested two different immobilization approaches (DIV and 5'exon) to ensure that Mss116 binding is not hindered by immobilization, despite the binding site is believed to be in DI. The determined K_D-values for both approaches are very similar and within the experimental error (Table 1, Figure S3, and S4). No significant changes in the binding of Mss116 were observed when the biotin tag was replaced with an amine tag. The tag exchange was necessary for the DNA linker hybridizing to DIV, and the target immobilization on a protein-free SPRi slide (Table 1 and Figure S5). The results demonstrated that neither DIV nor the 5'exon is involved in Mss116 binding, and DI is not concealed in both of the immobilization approaches, which is in line with previous findings that DI is the main interaction region for Mss116 (20). Additionally, the measured binding rates indicate a rapid binding of Mss116 (with a fast association rate constant) and a prolonged release.

SPRi-MALDI MS analysis of rough mitochondrial lysate from baker's yeast. Having shown that immobilization by either DIV or via the 5'exon does not affect Mss116 binding to ex^{41}-*Sc*.ai5γ-ex^{14}, we proceeded with SPRi-MALDI MS measurements and used the surface-immobilization via DIV. While it is known that members of DEAD-box helicases are often involved in multiple processes, such as mitochondrial intron splicing and transcription elongation (37), the interaction between *Sc*.ai5γ and other potential interactors has been poorly investigated. The hypothesis that group II introns and the spliceosome are evolutionarily related is well established. Following the theory of Galej and co-authors (38) that spliceosomal proteins gradually replaced intronic domains, we go a step further. We suggest that the mitochondrial group II intron forms a complex of RNA and a few co-factors, thus representing an evolutionary intermediate stage between the simple ribozymes in bacteria and the highly developed spliceosome in eukaryotes. We assume that besides Mss116, other regulating factors participate in the splicing process of *Sc*.ai5γ. To support this hypothesis, we combined SPRi with MALDI mass spectrometry for screening and identification of new potential intron binders. This method allows also the detection of interacting analytes in real time and the determination of association and dissociation constants.

Firstly, on-chip tryptic proteolysis needed to be optimized (Supporting Information, Figure S6). Secondly, by performing SPRi-MALDI MS analysis we faced another challenge. Although immobilization via biotin or amine tagged RNA resulted in only marginal differences in binding constants, it affected the MALDI MS analysis significantly. Biotinylated RNA is immobilized on SPRi slides coated with *ExtrAvidin*, a modification of avidin with high affinity and specificity to biotin. However, this causes too many disrupting, intense peaks in the mass spectrum (Figure S7 A and B) when

spots of interest are digested with trypsin. The replacement of the enzyme trypsin with AspN, to generate *ExtrAvidin*-peptides with higher m/z values did not improve the situation. In this case, autolysis products of AspN dominated the entire mass spectrum (Figure S7 C and D), even when the same low concentrations as for trypsin were used. Finally, to avoid interfering peaks, we used SPRi slides in the absence of any protein functionalization. We chose N-hydroxy succinimide (NHS) ester functionalized surfaces, which require free amine groups on the molecule for immobilization. Obtaining high-quality mass spectra from on-chip proteolysis of captured analytes (in the low fmol range) from arrayed SPRi slides is considered challenging. Using our optimized workflow, after the immobilization of the amine-tagged ex^{41}-*Sc*.ai5γ-ex^{14} (DIV), captured Mss116 could be identified after the injection of the pure protein, with a reasonably high number of fragments and a sequence coverage of 68 % from only 9.4 fmol (Figure 2 C and Figure S8).

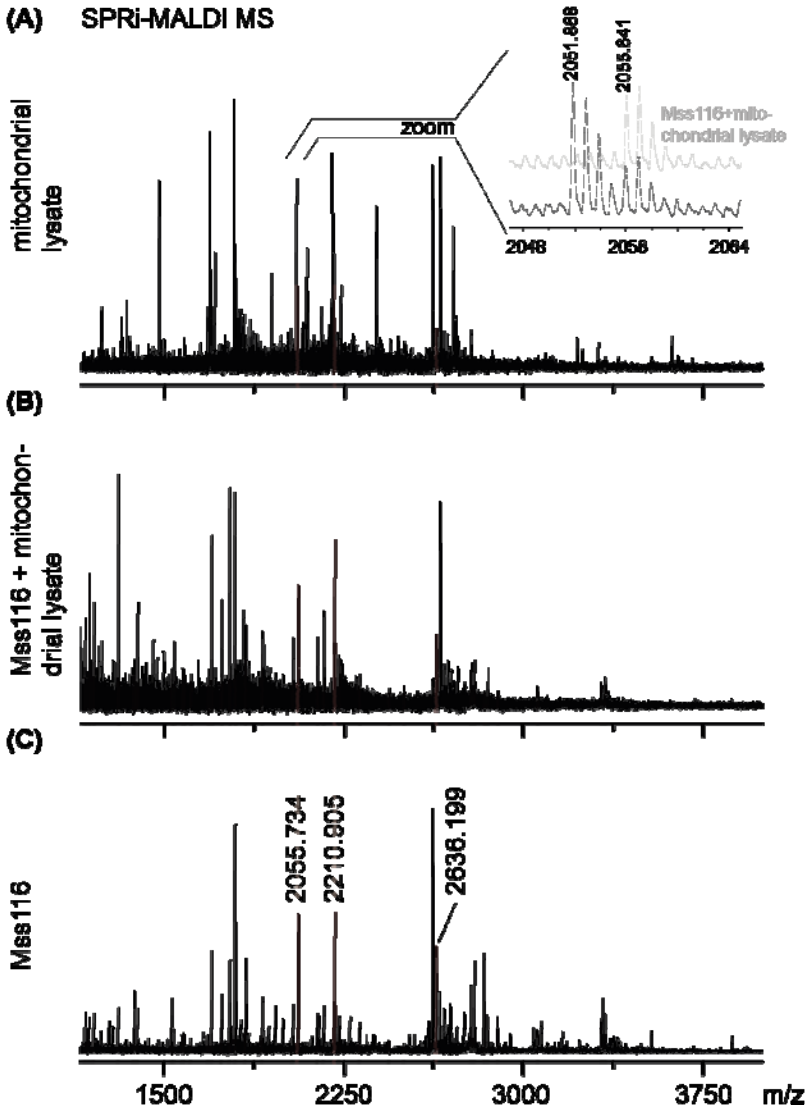

Figure 2. On-chip MALDI mass spectra after SPRi measurements and on-chip proteolysis (with reduction) after **(A)** the direct injection of a rough mitochondrial fraction lysate, **(B)** the injection of 250 nM Mss116 (causing saturation in the SPR sensorgram) and mitochondrial fraction without regeneration in between, and **(C)** the injection of Mss116 (135 nM). Grey bars mark the same peptides found in the spectra **B** and **C**, while light red highlighted peptides were found in all three experiments. A complete assignment of the peptide mass fingerprint from Mss116 **(C)** can be found in Figure S8 (Supporting Information). Assignments of the peaks from the lysate **(A)** are given in Table 2.

To investigate if proteins other than Mss116 interact with ex^{41}-*Sc*.ai5γ-ex^{14} we applied a rough mitochondrial lysate from yeast to the immobilized RNA. The MALDI MS experiment was performed after a single injection of the lysate and based on real-time detected plasmon curves, i.e., if an interaction is detected/not detected. The mass spectrum of the on-chip tryptically digested spots of interest revealed a

high number of peptides (Figure 2 A). A comparison between the peptide mass fingerprint spectrum of Mss116 (Figure 2 C) and the mitochondrial fraction (Figure 2 A) shows distinct differences, i.e., many peptides with different m/z values were observed, indicating that proteins other than Mss116 bind to ex[41]-*Sc*.ai5γ-ex[14]. Only three rather low-intensity peaks were observed, e.g., the signal at m/z 2055.841 (Figure 2 A, zoomed part), indicating binding of Mss116. A Mascot database query of the fragments shows that several other proteins interact with the target RNA as well. Based on peaks with a signal-to-noise ratio higher than 1.5 and a mass deviation of less than 190 ppm (as achieved with on-chip digested Mss116), we identified four distinct proteins, namely the pre-mRNA-splicing factor 8 (Prp8), DEAD-box protein 8 (Dbp8), mitochondrial ribosomal protein 13 (Mrp13) and a protein known as Cullin-3. The identity of the last two proteins was further verified by MS/MS measurements of selected ions. The MS/MS spectrum of ion m/z 1791.704 (Figure 3) confirmed the amino acid sequence AKLDEFLIYHKTDAK originating from Mrp13. The fragmentation of the ion m/z 2198.940 supports the presence of Cullin-3 (Figure S9).

Table 2. Captured and identified binders of ex[41]-*Sc*.ai5γ-ex[14] out of a rough mitochondrial lysate and on-chip proteolysis using MALDI MS (compare to Figure 2A). Peptides with their m/z value, number of missed cleavages (MC), signal-to-noise ratio (S/N), deviation from theoretical m/z (Δppm), and amino acid sequences are grouped into each identified protein resulting from a Mascot database request and peptide mass fingerprint.

m/z	MC	S/N	|Δppm|	amino acid sequence	protein
1125.491	0	13	30.2	NYYYLFDK	Pre-mRNA-splicing factor 8 Prp8
1475.688	1	27	140.2	SAIANTLLYLRLK	
1584.695	1	4	142.4	NDTKILVLALEDLK	
1687.934	0	32	72.5	WFLQHPDEEYPVK	
1828.810	1	5	139.3	GTIPLLERYIGNLITR	
2096.935	2	15	35.7	IINTHSDMASKMYNTDKK	
2236.929	2	10	122.7	YIGNLITRQFEGRSNEIVK	
2717.031	2	7	186.5	KYNVNISALTQTEIKDIILGQNIK	
3312.171	2	3	127.3	GILMASGSTTFTKVAAKWNTSLISLFTYFR	
3622.302	2	4	75.4	VAAKWNTSLISLFTYFREAIVATEPLLDILVK	
1339.568	0	10	144.1	IEYILVPEHVK	ATP-dependent RNA helicase Dbp8
1797.801	2	9	34.1	ESLMAMQKENFGERK	
1818.776	2	7	119.5	TARAGRIGDAISFVTQR	
1947.881	2	11	79.6	AGRIGDAISFVTQRDVSR	
1791.704	2	33	145.2	AKLDEFLIYHKTDAK	37S ribos. protein Mrp13
2779.206	2	4	119.1	AIWTYISPIHVQKMLTASFFKIGK	
3223.205	0	4	145.1	QIGFTPELTGLQPVDISLPDIPNSSSGAELK	
1708.723	0	12	62.1	SQHSFLESIDFGSVR	Cullin-3
2051.868	2	23	151.7	LSLTPSILKRSIQLLIEK	
2091.865	2	12	109.1	SYINKNAINIPFNEGNRK	
2198.940	1	29	36.9	EGALPSEYLSTYVDHCMKR	

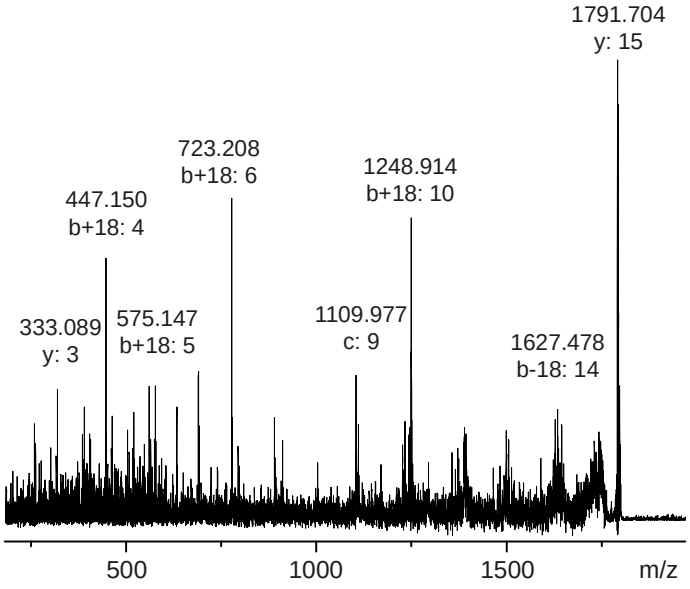

m/z	ion	position	amino acid sequence
333.089	y	1-3	AKL
359.077	x	1-3	
447.150	b+18	1-4	AKLD
461.088	x	1-4	
530.140	a	1-5	AKLDE
562.137	y	1-5	
575.147	b+18	1-5	
723.208	b+18	1-6	AKLDEF
1109.977	c	1-9	AKLDEFLIY
1248.914	b+18	1-10	AKLDEFLIYH
1627.478	b+18	1-14	AKLDEFLIYHKTDA
1746.350	a	1-15	AKLDEFLIYHKTDAK
1791.704	y	1-15	

Figure 3. SPRi-MALDI MS: On-chip MS/MS measurement of the peptide m/z 1791.704 (from Mrp13), which was detected after injecting a rough mitochondrial fraction lysate. A complete list with identified fragments (m/z values, cleavage site of the peptide ("ion"), positions of involved amino acids ("position") and amino acid sequence) is given in the table to the right of the spectrum.

To exclude non-specific adsorption resulting from the SPRi slide surface and thus false-positive signals, we used reference spots (without immobilized ex^{41}-*Sc*.ai5γ-ex^{14}) as controls. Here, no increasing signal in plasmon curves after the addition of the lysate or peptides from MALDI MS measurements were observed (not shown).

For further investigation of the potential binding sites of the identified proteins for ex^{41}-*Sc*.ai5γ-ex^{14}, we applied epitope blocking. Thereby, Mss116 was first injected to saturate its binding site on the RNA fixed on the SPR surface. Without regenerating the surface, the yeast mitochondrial lysate was subsequently added. The sensorgram signal increased only marginally compared to the direct injection of the mitochondrial fraction. The mass spectrum (Figure 2 B) shows mainly peaks corresponding to Mss116 and only a few others that are different from those of mitochondrial lysate only (Figure 2 A). This result suggests that all identified other proteins bind to a similar RNA region as Mss116, and the binding of Mss116 to the RNA is not competitive, as other proteins do not decisively displace Mss116. The obtained results demonstrate that the improved on-chip digestion workflow using SPRi-MALDI MS is a powerful tool for identifying new potential binders.

Discussion

Group II intron ribozymes are RNAs that undergo autocatalytic self-splicing. Self-splicing is thereby achieved solely by the complex RNA three-dimensional structure, which is defined by a multitude of tertiary contacts. In contrast, spliceosomal introns require and recruit the spliceosomal RNAs together with up to 80 proteins for splicing. Considering the large difference in the number of proteins involved between these splicing pathways and the evolutionary relationship between the spliceosome and group II introns, the questions arise whether also group II introns do need assistance from additional co-factors *in vivo* (beside Mss116). A recently emerging theory suggests that during evolution, proteins or ribonucleoproteins stepwise replaced structural elements of the intron (38), but so far, there is no experimental evidence of this. In this respect, organelle group II introns could represent an evolutionary intermediate between the bacterial introns and the complex eukaryotic spliceosome.

In the part of our study, we followed the binding kinetics of the natural co-factor Mss116 to ex^{41}-*Sc*.ai5γ-ex^{14} using SPRi technique and screened for new potential target RNA binders combining the SPRi with MALDI MS method. Mss116 is the only protein reported so far, which assist the folding of *Sc*.ai5γ *in vivo* and its subsequent splicing. Mss116 binds the three-way junction in DI of the ribozyme and initiate the folding of this large domain and induce the rearrangement of the remaining domains to achieve the fully functional native state (20). After evaluating two different immobilization approaches (DIV and 5'exon) it was demonstrated that neither DIV nor the 5'exon is involved in Mss116 binding. Note that DI is not hidden in both of the immobilization approaches, which correlates with previous findings that DI is the main interaction region for Mss116 (20). Additionally, determining the binding and unbinding constants of the protein revealed a very fast and tight binding of Mss116 to ex^{41}-*Sc*.ai5γ-ex^{14} and a very slow unbinding. Previous studies suggest that the dissociation of Mss116 from the RNA is driven by the hydrolysis of ATP (16,36). Although all experimental tests were performed in the presence of ATP, we could not observe the complete dissociation of the protein from ex^{41}-*Sc*.ai5γ-ex^{14}, and under our experimental conditions the protein remains bound to the target molecule.

Further we investigated for new potential binders to group II intron *Sc*.ai5γ, in addition to the well-known splicing co-factor Mss116, by screening a rough yeast mitochondrial lysate with SPRi-MALDI MS. Our screening experiments successfully revealed four potential binders to *Sc*.ai5γ, namely Dpb8, Prp8, Mrp13 and Cullin-3. The ribosomal, nucleolar protein Dbp8 is an ATP-dependent RNA helicase like Mss116 and is known to participate in the synthesis of the small ribosomal subunit, 18S rRNA (39). Both proteins belong to the superfamily 2 helicases and have high sequence similarity belonging to the class of DEAD-box proteins, that all share a highly conserved Walker motif (40). It has been shown

previously that unlike Mss116, Dbp8 does not influence the splicing of *Sc*.ai5γ due to the lack of an arginine-rich C-terminus (14). However, the function of Dbp8 in the *Sc*.ai5γ maturation process has not been further investigated, leaving the question about its binding property relevance unanswered. The pre-mRNA-splicing factor 8 (Prp8), is known to be part of the yeast spliceosomal core, and a key regulator in splicing intronic RNA in the nucleus by interacting with the catalytic RNA core, namely the 5'-and 3'-splice site and the essential branch point (41,42). Prp8 is made up of four domains, namely an RNA-binding domain, a reverse transcriptase-like domain, an RNaseH-like domain, and a C-terminus. (43,44). Structural and mechanistic evidence indicate that group II introns and the spliceosome are evolutionary related. In fact, the spliceosome appears to have evolved from group II introns (1,3,4). The identification of Prp8 as a binding partner to a group II intron strongly supports the relationship between both species and the hypothesis that group II introns are the ancestor of the spliceosome.

It has also been shown that numerous ribosomal proteins have similar structural properties (45-47), such as the mitochondrial ribosomal protein 13 (Mrp13). Mrp13 resembles the protruding β-finger domain (48), such as Mss116, containing hydrophilic residues that support the identification as a captured protein. Cullin-3 is described as a scaffold protein and a component of the protein degradation-related ubiquitylation pathway (49-51). However, neither specific nor non-specific interactions of Cullin-3 with intronic RNA have been described in the literature. The absence of a crystal structure of the intact protein prevents elucidating possible interaction sites as well as a comparison with known RNA-binding proteins. Nevertheless, Cullin-3, similar to Mss116, contains a comparable number of hydrophilic amino acids, which are important for RNA binding. All four newly identified proteins comprise RNA-binding properties that enable them to recognize certain RNA motifs, present in *Sc*.ai5γ.

Among these binders, the mitochondrial protein Mrp13 is of high interest due to its localization and possible function within the *Sc*.ai5γ maturation process. Indeed, the other three binding proteins have been reported (UniProt) to be located in the nucleus and to lack a mitochondrial signaling motif required for the transport of nuclear proteins into the mitochondria. However, there are other mechanisms known for delivery of cellular or nuclear proteins into mitochondria, rather than the signaling peptide pathway. Their presence in the mitochondria and their biological relevance and interaction with *Sc*.ai5γ *in vitro* and *in vivo* needs further investigations. The nucleolar protein Prp8, for instance, has sequence similarity with the catalytic domain of reverse transcriptase from bacterial group II intron encoded protein (44), which supports the result as a potential binding partner. It was reported that non-mitochondrial proteins, as well as proteins derived from species different than yeast, trigger the splicing in *Sc*.ai5γ (14) *in vitro*. Solem *et al.* (14) have shown that the cytoplasmic ATP-dependent helicase DED1 and Cyt-19 in *Neurospora crassa*, both members of the DEAD-box family, stimulate *Sc*.ai5γ splicing *in vitro*, but whether this is due

to sequence similarity to Mss116 and whether the interaction occurs *in vivo* is unknown. Additionally, these proteins are known to be multifunctional, and therefore it is not surprising that they can bind different kinds of RNAs (21,52,53). Group II introns do not share a common primary structure, but their secondary and tertiary structure is highly conserved among all species. *Sc*.ai5γ comprises structural similarities with other intronic RNAs, and its co-factor Mss116 shares common features with similar functioning RNA-binding proteins (54). Hence, the identification of four additional binding partners to *Sc*.ai5γ is the first experimental indication of other potential co-factors that may be involved in the group II intron splicing process *in vivo*.

The mitochondrial lysate, containing the four newly identified binding proteins were further analyzed in an epitope blocking experiment. For this, the binding site of the immobilized RNA was, in a first step, saturated with Mss116 and the mitochondrial lysate was subsequently injected. Proteolytic peptides of Mss116 dominated the mass spectrum, while none were detected from the lysate. There are two explanations for this finding: (i) the newly identified binders share the same RNA binding site with Mss116, which cannot be removed because being present in large excess, or (ii) binding of Mss116 to the RNA introduces structural changes that prevent other proteins from binding to their native site, different from the Mss116 binding site. The latter case would imply that the other four proteins possibly bind to the group II Intron not in the pre-spliced state but rather at a later stage of the splicing reaction. To identify specific binding regions, further experiments are required. Using different immobilization schemes of ex^{41}-*Sc*.ai5γ-ex^{14}, we could demonstrate that neither DIV nor the 5'exon is involved in Mss116 binding and that DI is accessible in each of the used immobilization schemes. These results are consistent with the previously proposed Mss116 binding site in *Sc*.ai5γ, namely DI (20).

RNA-binding proteins are usually grouped into either specific or non-specific binders, where the latter are still poorly understood. The question of how these proteins differentiate between binding sites is still unanswered. A good approach might be to investigate whether the binding is kinetically controlled. This would show differences in association and/or dissociation rate constants, while equilibrium dissociation constants (K_D) may have similar values. The demand for screening and high-throughput analysis tools, including non-targeted approaches, is steadily increasing. Our established SPRi-MALDI MS workflow can improve and promote this research. While only one RNA construct has been analyzed in this work, the investigation of crude lysate and the identification of specific RNA-binding proteins, strongly support the potential of coupling SPRi with MALDI MS as a powerful screening technique. The identification of the four new proteins binding to the yeast mitochondrial group II intron ribozyme *Sc*.ai5γ strongly supports the hypothesis that more than only one protein (Mss116) is required for self-splicing *in vivo*.

The present RNA – protein interaction study nicely demonstrates the potential of SPRi-MALDI MS as a general tool to identify such interactions, by using one of the largest ribozymes known (ex^{41}-*Sc*.ai5γ-ex^{14}) as a ligand. Non-targeted, non-covalent interactions are thereby also detected from complex mixtures of proteins, i.e., a cell lysate. For determining the identity of the binding partners, a complementary technique is adapted, in our case MALDI MS. Combining SPRi with MALDI MS in a unified workflow represents a powerful tool for identifying target binders from specific cell compartments. So far, similar investigations have only been carried out on known in protein-protein interactions (30,31). The on-chip workflow developed here generates high-quality mass spectra (including better S/N values), leading to enhanced confidence in protein identification. With the implementation of a reduction step prior to digestion and a proper amount of trypsin (see Experimental procedures), we were able to overcome the difficulties of identifying very low amounts of protein.

Experimental procedures

Materials. Trypsin Gold (mass spectrometry grade) was purchased from Promega. DNA linkers, oMGG03 and oMGG05, were ordered at IBA Lifesciences (Göttingen, Germany) and oMGG06 from Microsynth AG (Balgach, Switzerland). All sequences are given in the Supporting Information. Plasmids pJD20 and pHRH108 were kindly provided by A. M. Pyle, Yale University. All chemicals were ordered at the highest available grade from Acros, Fluka, ABCR-Chemicals, or Merck. All solutions for SPR measurements were prepared using DNase, RNase, Protease free water (Molecular Biology Reagent, Sigma-Fine Chemicals).

RNA preparation. The group IIB intron *Sc*.ai5γ DNA, flanked by a 41 nucleotide (nt) and 14 nt long 5'-exon and 3'-exon respectively, was generated by polymerase chain reaction (PCR) amplification using plasmid pJD20 as a template (55,56), and primers oMGG01 and oSPA37, yielding finally plasmid pMGG01. The pMGG01 DNA construct was *in vitro* transcribed using an in-house produced T7 RNA polymerase. The RNA transcript (referred to as ex^{41}-*Sc*.ai5γ-ex^{14} – superscript numbers indicate the number of nucleotides from the flanking exons) was purified on a 8 % denaturing polyacrylamide gel, extracted by electroelution in Tris-borate-EDTA (TBE, pH 8.3) buffer, ethanol precipitated and finally dissolved in distilled water (adapted from Gallo *et al*.) (57).

Protein production. The mitochondrial protein Mss116 (UniProt identifier P15424) DNA was derived from pHRH108 (34). The full-length Mss116 DNA, lacking the mitochondrial localization signal, was delivered in a commercially available pET-SUMO champion vector (Invitrogen), which contains an N-

terminal His(6)tag, followed by a SUMO tag sequence. Protein expression and purification were performed as described (14,58), with the following modifications: The protein was expressed in BL21 competent cells. The bacterial cells were resuspended in a lysis buffer (50 mM Tris-HCl pH 7.5, 500 mM NaCl, 10 mM imidazole, 10 % sucrose, 5 mM β-mercaptoethanol, 1 % IGEPAL-630 and 10 % glycerol). Cell lysis was performed by shock freeze in liquid nitrogen, thawing on ice, and sonication. The lysate was centrifuged at 20'000 *g* at 4 °C for 30 min. The supernatant was filtered and purified by gravity flow Ni-NTA affinity chromatography. The chromatographic columns were filled with 2.5 mL Nickel-Chelating-Resin 50 % slurry in 20 % ethanol (G-Bioscience), washed with 10 column volumes lysis buffer, and eluted in 2 mL fractions in a lysis buffer, containing 250 mM imidazole. Mss116 protein was further purified by FPLC Superdex 200 (GE Healthcare), the protein purity was checked by sodium dodecyl sulfate-polyacrylamide gel electrophoresis (SDS PAGE) (detailed results are in the Supporting Information Figure S1 and Figure S2), and MS. Aliquots were stored at -20 °C in a storage buffer (50 mM Tris-HCl pH 7.5, 500 mM NaCl, 1 mM DTT and 10 % glycerol). Protein activity was measured by the ATPase activity assay (Sigma-Aldrich) as described by the manufacturer.

On-plate digestion optimization. To improve the quality of on-chip tryptic digestion of captured proteins after SPRi measurements, bovine serum albumin (BSA) was used in varying amounts (1 pmol, 100 fmol, and 10 fmol) as a control protein. All steps were performed without explicitly mixing the solution on the plate. For reduction, DL-dithiothreitol (DTT) and Tris(2-carboxyethyl)phosphine hydrochloride (TCEP) were used at different concentrations (50 mM, 10 mM, 5 mM, 1 mM, 0.5 mM, 0.1 mM and 0.01 mM in 25 mM NH_4HCO_3, pH 8.5). 1 µL of reducing agent was spotted on top of the BSA spots and allowed to react for 1 h, 40 min, 30 min, 20 min, or 10 min at 37 °C. For alkylation, 1 µL of iodoacetamide solution of varying concentrations (5 mM, 1 mM, 0.5 mM, and 0.1 mM) was spotted and incubated for 1 h at 25 °C in the dark. 1 µL of reducing agent was added with the same concentration as the used iodoacetamide (in 25 mM NH_4HCO_3 buffer, pH 8.5) to quench excess iodoacetamide. Subsequently, 1 µL of trypsin solution (5 ng/µL) was added to each spot and incubated at 37 °C for 10 min. Finally, the spots were dried at 37 °C and matrix solution (7 mg/mL α-CHCA in 50 % acetonitrile/water with 0.3 % trifluoroacetic acid (TFA)) was spotted. Detailed results are given in Supporting information (p. S8ff).

Surface Plasmon Resonance Imaging. All SPRi measurements were carried out using a commercial SPRi-Plex II instrument and standard gold SPRi slides for amine or biotin coupling, respectively (Horiba France, Palaiseau, France). RNA and BSA, as controls, were immobilized by spotting 0.3 µL (0.1 mg/mL) manually on the chip in a 4 x 4 spot array pattern. Blocking buffer consisted of 1 M aqueous ethanolamine (pH 9.0) or 10 µg/mL biotin, respectively. For joining the SPRi slide with the surface of a

glass prism with a high refractive index, a thin film of index-matching oil was used to connect both surfaces. SPRi experiments were performed at 25 °C with buffer containing 500 mM KCl, 80 mM MOPS (pH 6.9), 10 mM $MgCl_2$ and 10 µM ATP, respectively, with a flow rate of 50 µL/min and a 150 µL injection volume. For surface regeneration between measurements, 100 mM glycine hydrochloride ($H_2NCH_2CO_2H$ □HCl, pH 2.0) was used.

Measured kinetic curves were evaluated using the Scrubber Gen2 software. For calculating the kinetic and binding constants k_{on}, k_{off}, and K_D, a classical Langmuir model was applied.

In preparation for the immobilization step, RNA was hybridized with short DNA linkers (oMGG03, oMGG05 or oMGG06) in dH_2O in a 1:1 ratio by heating for 3 min at 90 °C and then slowly cooling down to 25 °C.

MALDI MS. For MALDI MS measurements, a tryptic digest was performed directly on the chip surface, after being removed from the SPRi instrument and air-dried. The target proteins were reduced for 1 h at 37 °C with 500 pmol of aqueous TCEP in 25 mM ammonium bicarbonate, pH 8.5. The addition of 25 mM ammonium bicarbonate solution prevents the sample from drying out. Trypsin (5 ng/µL in 10 mM ammonium bicarbonate, pH 8.3) was spotted (0.3 µL) onto the region of interest and kept in a humid atmosphere at 37 °C for 10 min. Finally, after the spots had dried and digestion had stopped, MALDI matrix was applied (0.1 µL of 7 mg/mL α-cyano-4-hydroxycinnamic acid (α-CHCA) in 50 % acetonitrile/water with 0.3 % TFA). For MALDI MS measurements, the SPRi slide was mounted directly into a custom-made SPRi-MALDI adapter. Mass spectra were obtained with an Ultraflex II MALDI-TOF (Bruker Daltonics, Bremen, Germany), which is equipped with a "smartbeam" laser working with a 66.7 Hz repetition rate, using the following parameter settings: positive ion reflectron mode, acceleration voltage: 25 kV, delayed extraction time: 20 ns, laser fluence: just above the desorption/ionization threshold, number of laser shots: 1'500-2'500 (averaged and acquired at random sample positions). All mass spectra were smoothed, baseline-subtracted, and externally calibrated with a standard peptide calibration mix I (LaserBio Labs), which was also spotted onto the SPRi slide. Tryptic peptides were identified with the Biotools software (Bruker Daltonics) and Mascot software (Matrix Science Limited).

Preparation of rough mitochondrial fractions. The protocol was adapted from Glick and Pon (59). Harvested yeast cells were washed with water and collected by centrifugation at 4'000 *g* for 5 min at 25 °C. The pellet was resuspended in 100 mM Tris buffer (pH 8.4) and 10 mM DTT for 10 min at 30 °C and centrifuged at 2'000 *g* for 5 min at 25 °C. After washing with 1.2 M sorbitol and centrifuging for 5 min at 4'000 *g* at 25 °C, the pellet was resuspended in 40 mL buffer containing 1.2 M sorbitol, 20 mM KH_2PO_4 (pH 7.4) and 3 mg/g Zymolyase and incubating for 60 min at 30 °C in a water bath. All the subsequent

procedures were performed at 0-4 °C. The suspension was centrifuged for 5 min at 2'000 *g*, the supernatant removed, and 100 mL homogenization buffer (10 mM Tris, pH 7.4, 1 mM EDTA, 0.2 % BSA, 1 mM PMSF and 0.6 M sorbitol) was added to the pellet and mixed thoroughly. The suspension was homogenized using a Dounce homogenizer and centrifuged for 5 min at 4'000 *g*. The supernatant was saved and additionally centrifuged for 12 min at 7'000 *g*. The resulting mitochondrial pellet was resuspended in 1 mL buffer containing 500 mM KCl, 80 mM MOPS (pH 6.9), 10 mM $MgCl_2$, and 0.5 % Triton-X.

Author Contributions - The manuscript was written through the contributions of all authors. All authors have given approval to the final version of the manuscript. UA and MGG contributed equally to this work. UA, MGG, and SZP designed the experiments. MGG and SZP developed different immobilization approaches. MGG produced and purified the functional RNA and its co-factor Mss116. UA performed the SPRi-MALDI MS experiments and the corresponding data analysis.

Supporting Information - Supporting information includes the amino acid sequence of Mss116, FPLC elution profile of the purified protein Mss116 , SDS PAGE gel image of the purified Mss116, the sequences of the DNA oligonucleotides used for different immobilization strategies, the RNA sequence of the full-length group IIB intron with the shortened flanking exons ex^{41}-*Sc*.ai5γ-ex^{14}, and the primers used for the DNA construct amplification by PCR. SPR measurements with and without ATP for both immobilization strategies; description of on-chip digestion optimization; MALDI mass spectra showing the effect of *ExtrAvidin*-coated SPRi surfaces; MALDI mass spectrum after SPRi measurement from captured Mss116 with corresponding fragments, MS/MS measurement of the peptide m/z 2198.940 detected after injecting a rough mitochondrial fraction lysate.

Funding Sources - We thank Horiba Jobin Yvon for the loan of an SPRi instrument and Bruker Daltonics, Horiba Jobin Yvon for jointly funding 1.5 years of a Ph.D. studentship for UA, and Forschungskredit FK 16-083 to MGG. This work was financially supported by UZH (to RKOS) and by the Swiss National Science Foundation, grants # 200020_159929 (to RZ), and 200020_165868/1 (to RKOS).

Notes - The authors declare no competing financial interest. The original data used in this publication are made available in a curated data archive at ETH Zurich (https://www.researchcollection.ethz.ch) under the DOI 10.3929/ethz-b-000350562.

Acknowledgments - We thank Manuela Zimmermann (Bachelor Student at Prof. R.K.O. Sigel group, Department of Chemistry, University of Zurich) for the production of Mss116. We thank Dr. Carmelina Petrungaro (group of Prof. Benoît Kornmann, Institute of Biochemistry, ETH Zurich) for kindly cultivating *Saccharomyces cerevisiae* cells and for the introduction into the preparation of mitochondrial lysate. We also thank the Molecular and Biomolecular Analysis Service (MoBiAS, ETH Zurich) for access to the MALDI MS instrument and productive discussions.

Abbreviations - α-CHCA, α-cyano-4-hydroxycinnamic acid; ATP, adenosine 5'-triphosphate; BSA, bovine serum albumin; dH_2O, distilled water; DNA, desoxyribonucleic acid; EDTA, ethylenediaminetetraacetic acid; FPLC, fast protein liquid chromatography; His, histidine; IGEPAL-630, detergent (registered trademark); nt, nucleotide; MALDI MS, matrix-assisted laser desorption/ionization mass spectrometry; MOPS, 3-(N-morpholino)propanesulfonic acid; Ni-NTA, nickel-nitrilotriacetic acid; PCR, polymerase chain reaction; PMSF, phenylmethylsulfonyl fluoride; RNA, ribonucleic acid; Sc, Saccharomyces cerevisiae; SPRi, surface plasmon resonance imaging; SUMO, Small Ubiquitin-like Modifier; TBE, Tris-borate-EDTA; TCEP, tris(2-carboxyethyl)phosphine; TFA, trifluoroacetic acid; Tris, tris(hydroxymethyl)aminomethane.

References

1. Fica, S. M., Tuttle, N., Novak, T., Li, N.-S., Lu, J., Koodathingal, P., Dai, Q., Staley, J. P., and Piccirilli, J. A. (2013) RNA catalyses nuclear pre-mRNA splicing. *Nature* **503**, 229-234
2. Cate, J. H. D. (2016) A Big Bang in spliceosome structural biology. *Science* **351**, 1390
3. Cech, T. R. (1986) The generality of self-splicing RNA: Relationship to nuclear mRNA splicing. *Cell* **44**, 207-210
4. Zimmerly, S., and Semper, C. (2015) Evolution of group II introns. *Mobile DNA* **6**, 7
5. Sigel, R. K. O. (2005) Group II intron ribozymes and metal ions – A delicate relationship. *Eur. J. Inorg. Chem.* **2005**, 2281-2292
6. Donghi, D., and Schnabl, J. (2015) Multiple roles of metal ions in large RNAs. in *Metal Ions Life Sci. 9*. pp 197-234
7. Qu, G., Kaushal, P. S., Wang, J., Shigematsu, H., Piazza, C. L., Agrawal, R. K., Belfort, M., and Wang, H.-W. (2016) Structure of a group II intron in complex with its reverse transcriptase. *Nat. Struct. Mol. Biol.* **23**, 549
8. Zhao, C., and Pyle, A. M. (2017) Structural insights into the mechanism of group II intron splicing. *Trends Biochem. Sci* **42**, 470-482
9. Michel, F., Jacquier, A., and Dujon, B. (1982) Comparison of fungal mitochondrial introns reveals extensive homologies in RNA secondary structure. *Biochimie* **64**, 867-881
10. Toor, N., Keating, K. S., Taylor, S. D., and Pyle, A. M. (2008) Crystal structure of a self-spliced group II intron. *Science* **320**, 77
11. Fedorova, O., and Zingler, N. (2007) Group II introns: structure, folding and splicing mechanism. *Biol. Chem.* **388**, 665
12. Séraphin, B., Simon, M., Boulet, A., and Faye, G. (1989) Mitochondrial splicing requires a protein from a novel helicase family. *Nature* **337**, 84-87
13. Huang, H.-R., Rowe, C. E., Mohr, S., Jiang, Y., Lambowitz, A. M., and Perlman, P. S. (2005) The splicing of yeast mitochondrial group I and group II introns requires a DEAD-box protein with RNA chaperone function. *Proc. Natl. Acad. Sci. USA* **102**, 163
14. Solem, A., Zingler, N., and Pyle, Anna M. (2006) A DEAD protein that activates intron self-splicing without unwinding RNA. *Mol. Cell* **24**, 611-617
15. Zingler, N., Solem, A., and Pyle, A. M. (2010) Dual roles for the Mss116 cofactor during splicing of the ai5γ group II intron. *Nucleic Acids Res.* **38**, 6602-6609
16. Fedorova, O., Solem, A., and Pyle, A. M. (2010) Protein-facilitated folding of group II intron ribozymes. *J. Mol. Biol.* **397**, 799-813
17. Potratz, J. P., Del Campo, M., Wolf, R. Z., Lambowitz, A. M., and Russell, R. (2011) ATP-dependent roles of the DEAD-Box protein Mss116p in group II intron splicing in vitro and in vivo. *J. Mol. Biol.* **411**, 661-679
18. Del Campo, M., Mohr, S., Jiang, Y., Jia, H., Jankowsky, E., and Lambowitz, A. M. (2009) Unwinding by local strand separation is critical for the function of DEAD-box proteins as RNA chaperones. *J. Mol. Biol.* **389**, 674-693

19. Karunatilaka, K. S., Solem, A., Pyle, A. M., and Rueda, D. (2010) Single-molecule analysis of Mss116-mediated group II intron folding. *Nature* **467**, 935-939

20. Fedorova, O., and Pyle, A. M. (2012) The brace for a growing scaffold: Mss116 protein promotes RNA folding by stabilizing an early assembly intermediate. *J. Mol. Biol.* **422**, 347-365

21. Halls, C., Mohr, S., Del Campo, M., Yang, Q., Jankowsky, E., and Lambowitz, A. M. (2007) Involvement of DEAD-box proteins in group I and group II intron splicing. Biochemical characterization of Mss116p, ATP hydrolysis-dependent and -independent mechanisms, and general RNA chaperone activity. *J. Mol. Biol.* **365**, 835-855

22. Krone, J. R., Nelson, R. W., Dogruel, D., Williams, P., and Granzow, R. (1997) BIA/MS: Interfacing biomolecular interaction analysis with mass spectrometry. *Anal. Biochem.* **244**, 124-132

23. Nelson, R. W., Krone, J. R., and Jansson, O. (1997) Surface plasmon resonance biomolecular interaction analysis mass spectrometry. 1. Chip-based analysis. *Anal. Chem.* **69**, 4363-4368

24. Nelson, R. W., and Krone, J. R. (1999) Advances in surface plasmon resonance biomolecular interaction analysis mass spectrometry (BIA/MS). *J. Mol. Recognit.* **12**, 77-93

25. Mattei, B. C., Felice; Roepstorff, Peter. (2001) The interaction between endopolygalacturonase from Fusarium moniliforme and PGIP from Phaseolus vulgaris studied by surface plasmon resonance and mass spectrometry. *Comp. Funct. Genom.* **2**, 359-364

26. Bouffartigues, E., Leh, H., Anger-Leroy, M., Rimsky, S., and Buckle, M. (2007) Rapid coupling of Surface Plasmon Resonance (SPR and SPRi) and ProteinChip™ based mass spectrometry for the identification of proteins in nucleoprotein interactions. *Nucleic Acids Res.* **35**, e39-e39

27. Treitz, G., Gronewold, T. M. A., Quandt, E., and Zabe-Kühn, M. (2008) Combination of a SAW-biosensor with MALDI mass spectrometric analysis. *Biosens. Bioelectron.* **23**, 1496-1502

28. Nedelkov, D., and Nelson, R. W. (2000) Practical considerations in BIA/MS: optimizing the biosensor–mass spectrometry interface. *J. Mol. Recognit.* **13**, 140-145

29. Nelson, R. W., Nedelkov, D., and Tubbs, K. A. (2000) Biomolecular interaction analysis mass spectrometry. *Anal. Chem.* **72**, 404 A-411 A

30. Anders, U., Schaefer, J. V., Hibti, F.-E., Frydman, C., Suckau, D., Plückthun, A., and Zenobi, R. (2017) SPRi-MALDI MS: characterization and identification of a kinase from cell lysate by specific interaction with different designed ankyrin repeat proteins. *Anal. Bioanal. Chem.* **409**, 1827-1836

31. Musso, J., Buchmann, W., Gonnet, F., Jarroux, N., Bellon, S., Frydman, C., Brunet, D.-L., and Daniel, R. (2015) Biomarkers probed in saliva by surface plasmon resonance imaging coupled to matrix-assisted laser desorption/ionization mass spectrometry in array format. *Anal. Bioanal. Chem.* **407**, 1285-1294

32. Bellon, S., Buchmann, W., Gonnet, F., Jarroux, N., Anger-Leroy, M., Guillonneau, F., and Daniel, R. (2009) Hyphenation of surface plasmon resonance imaging to matrix-assisted laser desorption ionization mass spectrometry by on-chip mass spectrometry and tandem mass spectrometry analysis. *Anal. Chem.* **81**, 7695-7702

33. Kim, Y. E., Yi, S. Y., Lee, C.-S., Jung, Y., and Chung, B. H. (2012) Gold patterned biochips for on-chip immuno-MALDI-TOF MS: SPR imaging coupled multi-protein MS analysis. *Analyst* **137**, 386-392

34. Mohr, G., Del Campo, M., Mohr, S., Yang, Q., Jia, H., Jankowsky, E., and Lambowitz, A. M. (2008) Function of the C-terminal domain of the DEAD-box protein Mss116p analyzed in vivo and in vitro. *J. Mol. Biol.* **375**, 1344-1364

35. Grohman, J. K., Del Campo, M., Bhaskaran, H., Tijerina, P., Lambowitz, A. M., and Russell, R. (2007) Probing the mechanisms of DEAD-box proteins as general RNA chaperones: the C-terminal domain of CYT-19 mediates general recognition of RNA. *Biochemistry* **46**, 3013-3022

36. Liu, F., Putnam, A., and Jankowsky, E. (2008) ATP hydrolysis is required for DEAD-box protein recycling but not for duplex unwinding. *Proc. Natl. Acad. Sci.* **105**, 20209

37. De Silva, D., Poliquin, S., Zeng, R., Zamudio-Ochoa, A., Marrero, N., Perez-Martinez, X., Fontanesi, F., and Barrientos, A. (2017) The DEAD-box helicase Mss116 plays distinct roles in mitochondrial ribogenesis and mRNA-specific translation. *Nucleic Acids Res.* **45**, 6628-6643

38. Galej, W. P., Toor, N., Newman, A. J., and Nagai, K. (2018) Molecular mechanism and evolution of nuclear pre-mRNA and group II intron splicing: insights from cryo-electron microscopy structures. *Chem. Rev.* **118**, 4156-4176

39. Daugeron, M.-C., and Linder, P. (2001) Characterization and mutational analysis of yeast Dbp8p, a putative RNA helicase involved in ribosome biogenesis. *Nucleic Acids Res.* **29**, 1144-1155

40. Granneman, S., Bernstein, K. A., Bleichert, F., and Baserga, S. J. (2006) Comprehensive mutational analysis of yeast DEXD/H box RNA helicases required for small ribosomal subunit synthesis. *Mol. Cell. Biol.* **26**, 1183

41. Grainger, R. J., and Beggs, J. D. (2005) Prp8 protein: at the heart of the spliceosome. *RNA (New York, N.Y.)* **11**, 533-557

42. Will, C. L., and Lührmann, R. (2011) Spliceosome structure and function. *CSH Perspect. Biol.* **3**

43. Dlakić, M., and Mushegian, A. (2011) Prp8, the pivotal protein of the spliceosomal catalytic center, evolved from a retroelement-encoded reverse transcriptase. *RNA* **17**, 799-808

44. Galej, W. P., Oubridge, C., Newman, A. J., and Nagai, K. (2013) Crystal structure of Prp8 reveals active site cavity of the spliceosome. *Nature* **493**, 638

45. Yang, K., Zhang, L., Xu, T., Heroux, A., and Zhao, R. (2008) Crystal structure of the beta-finger domain of Prp8 reveals analogy to ribosomal proteins. *Proc. Natl. Acad. Sci. USA* **105**, 13817-13822

46. Ban, N., Nissen, P., Hansen, J., Moore, P. B., and Steitz, T. A. (2000) The complete atomic structure of the large ribosomal subunit at 2.4 Å resolution. *Science* **289**, 905

47. Wimberly, B. T., Brodersen, D. E., Clemons Jr, W. M., Morgan-Warren, R. J., Carter, A. P., Vonrhein, C., Hartsch, T., and Ramakrishnan, V. (2000) Structure of the 30S ribosomal subunit. *Nature* **407**, 327

48. Desai, N., Brown, A., Amunts, A., and Ramakrishnan, V. (2017) The structure of the yeast mitochondrial ribosome. *Science* **355**, 528

49. Ribar, B., Prakash, L., and Prakash, S. (2007) ELA1 and CUL3 are required along with ELC1 for RNA polymerase II polyubiquitylation and degradation in DNA-damaged yeast cells. *Mol. Cell. Biol.* **27**, 3211-3216

50. Cheng, J., Guo, J., Wang, Z., North, B. J., Tao, K., Dai, X., and Wei, W. (2018) Functional analysis of Cullin 3 E3 ligases in tumorigenesis. *BBA-Rev. Cancer* **1869**, 11-28

51. Canning, P., Cooper, C. D. O., Krojer, T., Murray, J. W., Pike, A. C. W., Chaikuad, A., Keates, T., Thangaratnarajah, C., Hojzan, V., Marsden, B. D., Gileadi, O., Knapp, S., von Delft, F., and Bullock, A. N. (2013) Structural basis for Cul3 protein assembly with the BTB-Kelch family of E3 ubiquitin ligases. *J. Biol. Chem.* **288**, 7803-7814

52. De Silva, D., Fontanesi, F., and Barrientos, A. (2013) The DEAD box protein Mrh4 functions in the assembly of the mitochondrial large ribosomal subunit. *Cell Metab.* **18**, 712-725

53. Tu, Y.-T., and Barrientos, A. (2015) The human mitochondrial DEAD-box protein DDX28 resides in RNA granules and functions in mitoribosome assembly. *Cell Rep.* **10**, 854-864

54. Dreyfuss, G., Kim, V. N., and Kataoka, N. (2002) Messenger-RNA-binding proteins and the messages they carry. *Nat. Rev. Mol. Cell Bio.* **3**, 195

55. Daniels, D. L., Michels Jr, W. J., and Pyle, A. M. (1996) Two competing pathways for self-splicing by group II introns: A quantitative analysis of in vitro reaction rates and products. *J. Mol. Biol.* **256**, 31-49

56. Jarrell, K. A., Peebles, C. L., Dietrich, R. C., Romiti, S. L., and Perlman, P. S. (1988) Group II intron self-splicing. Alternative reaction conditions yield novel products. *J. Biol. Chem.* **263**, 3432-3439

57. Gallo, S., Furler, M., and Sigel, R. K. O. (2005) In vitro transcription and purification of RNAs of different size. *CHIMIA* **59**, 812-816

58. Cao, W., Coman, M. M., Ding, S., Henn, A., Middleton, E. R., Bradley, M. J., Rhoades, E., Hackney, D. D., Pyle, A. M., and De La Cruz, E. M. (2011) Mechanism of Mss116 ATPase reveals functional diversity of DEAD-box proteins. *J. Mol. Biol.* **409**, 399-414

59. Glick, B. S., and Pon, L. A. (1995) [14] Isolation of highly purified mitochondria from Saccharomyces cerevisiae. in *Methods Enzymol.*, Academic Press. pp 213-223